INTERNATIONAL JOURNAL OF TECHNO-ENGINEERING
IJTE

ISSN: 2057-5688

Multiple-Input Multiple-Output OFDM with Index Modulation for Next Generation Wireless Networks

VEMULA NAGARJUNA [1], M PARAMESWARARAO [2]
[1]Assistant professor, [2] Assistant professor
Department of Electronics and Communication Engineering
ECE Department, Sri *Mittapalli College* of *Engineering*, *Guntur*, *Andhra Pradesh*-522233

Abstract--Multiple-input multiple-output orthogonal frequency division multiplexing with index modulation (MIMO-OFDM-IM) is a novel multicarrier transmission technique which has been proposed recently as an alternative to classical MIMO-OFDM. In this scheme, OFDM with index modulation (OFDMIM) concept is combined with MIMO transmission to take advantage of the benefits of these two techniques. In this paper, we shed light on the implementation and error performance analysis of the MIMO-OFDM-IM scheme for next generation 5G wireless networks. Maximum likelihood (ML), near-ML, simple minimum mean square error (MMSE) and ordered successive interference cancellation (OSIC) based MMSE detectors of MIMO-OFDM-IM are proposed and their theoretical performance is investigated. It has been shown via extensive computer simulations that MIMO-OFDM-IM scheme provides an interesting trade-off between error performance and spectral efficiency as well as it achieves considerably better error performance than classical MIMO-OFDM using different type detectors and under realistic conditions.

Index terms--OFDM, index modulation, MIMO systems, maximum likelihood (ML) detection, minimum mean square error (MMSE) detection, V-BLAST, 5G wireless networks.

I. INTRODUCTION

Orthogonal frequency division multiplexing (OFDM) is one of the most popular multi-carrier transmission techniques to satisfy the increasing demand for high data rate wireless communications

systems. OFDM technologies have become an integral part of many standards such as Long Term Evolution (LTE), IEEE 802.11x wireless local area network (LAN), digital video broadcasting (DVB) and IEEE 802.16e-WiMAX due to their efficient implementation
and robustness to inter-symbol interference.

Multiple-input multiple-output (MIMO) transmission techniques have been widely studied over the past decade due to their advantages over single antenna systems such as improved data rate and energy efficiency. Spatial modulation (SM), which is based on the transmission of information bits by means of the indices of the active transmit antennas of a MIMO system [1], is one of the promising MIMO solutions towards spectral and energy-efficient next generation communications systems [2]. SM has attracted significant attention by the researchers over the past few years [3]–[8] and it is still a hot topic in wireless communications [9].

OFDM with index modulation (OFDM-IM) [10] is a novel multicarrier transmission technique which has been proposed as an alternative to classical OFDM. Inspiring from the SM concept, in OFDM-IM, index modulation techniques are applied for the indices of the available subcarriers of an OFDM system. In OFDM-IM scheme, only a subset of available subcarriers are selected as active according to the information bits, while the remaining inactive subcarriers are set zero. In other words, the information is transmitted not only by the data symbols selected from M-ary signal constellations, but also by the indices of the active subcarriers. Unlike classical OFDM, the number of active subcarriers can be adjusted in the OFDM-IM scheme, and this
flexibility in the system design provides an interesting trade-off between error performance and spectral efficiency. Furthermore, it has been shown that OFDM-IM has the potential to achieve a better error performance than classical OFDM for low-to-mid spectral efficiency values. Due to its adjustable number of active subcarriers, OFDM-IM can be a possible candidate not only for high-speed wireless communications systems but also for machine-to-machine (M2M) communications systems which require low power consumption.

Subcarrier index modulation concept for OFDM [10]–[12] has attracted significant attention from the researchers over the past two years and it has been investigated in some very recent studies [13]–[22]. A tight approximation for the error performance of OFDM-IM is given in [13]. By the selection of active subcarriers in a more flexible way to further increase the spectral efficiency, OFDM-IM scheme is generalized in [14]. The problem of the selection of optimal number of active subcarriers is investigated in [15] and [16]. In [17], subcarrier level block interleaving is introduced for OFDM-IM in order to improve its error performance by taking advantage of uncorrelated subcarriers. In [18], OFDM-IM with interleaved grouping is adapted to vehicular communications. OFDM-IM is combined with coordinate interleaving principle in [19] to obtain additional diversity gains. More recently, it has been proved that OFDM-IM and its variants outperform the classical OFDM in terms of ergodic achievable rate [20] and coding gain [21].

Considering the advantages of OFDM and MIMO transmission techniques, the combination of them unsurprisingly appears as a strong alternative for 5G and beyond wireless networks [23]. MIMO-OFDM-IM, which is obtained by the combination of MIMO and OFDM-IM transmission techniques, is a recently proposed high-performance multicarrier transmission technology and can be considered as a possible alternative to classical MIMO-OFDM [22]. In this scheme, each transmit antenna transmits its own OFDM-IM frame to boost the data rate and at the receiver side, these frames are separated and demodulated using a novel sequential minimum mean square error (MMSE) detector which considers the statistics of the MMSE filtered received signals. However, since different applications have different error performance and decoding complexity constraints, the design and analysis of different type of detectors remain an open problem for the MIMO-OFDM-IM scheme.

In this paper, we deal with the implementation and error performance analysis of the MIMOOFDM-IM scheme for different type of detectors and active indices selection methods under realistic conditions. First, the maximum likelihood (ML) detector of the MIMO-OFDM-IM scheme is investigated to benefit from the diversity gain of MIMO systems and its average bit error probability (ABEP) is derived by the calculation of pairwise error probability (PEP) of the MIMO-OFDM-IM subblocks. Second, in order to reduce the decoding complexity of the bruteforce ML detector of the MIMO-OFDM-IM scheme, a novel low complexity near-ML detector is proposed which is shown to provide better bit error rate (BER) performance than V-BLAST type classical MIMO-OFDM for different configurations. Third, a simple MMSE detection algorithm is proposed and its theoretical ABEP is derived to shed light on

ISSN: 2057-5688

the performance of MIMOOFDM-IM for MMSE detection. Then, a novel ordered successive interference cancellation (OSIC) based sequential MMSE detector is proposed for MIMO-OFDM-IM. Finally, the error performance of MIMO-OFDM-IM is evaluated for a realistic LTE channel model and under channel estimation errors. It has been shown via computer simulations that MIMO-OFDM-IM can be a strong alternative to classical MIMO-OFDM due to its improved BER performance

and flexible system design.

The rest of the paper is organized as follows. In Section II, the system model of MIMO-

OFDM-IM is presented. In Sections III and IV, we deal with ML and MMSE detection of the MIMO-OFDM-IM scheme and provide our theoretical results, respectively. Simulation results

are provided in Section V. Finally, Section VI concludes the paper[1].

II. MIMO-OFDM-IM AT A GLANCE

1

The block diagram of the MIMO-OFDM-IM transceiver [22] is given in Fig. 1, where the concept of OFDM-IM, which is shown in Fig. 2, is extended to a MIMO configuration. A MIMO system with T transmit and R receive antennas is assumed. As seen from Fig. 1, a total of mT information bits enter the MIMO-OFDM-IM transmitter for the transmission of each MIMO-OFDM-IM frame. These mT bits are first split into T groups and the corresponding m bits are processed in each branch of the transmitter by the OFDM index modulators as shown in Fig. 2. Unlike the classical OFDM, these m bits are used not only in M-ary modulation

but also in the selection of the indices of active subcarriers and the $N_F \times 1$ OFDM-IM block

$\mathbf{x}_t = x_t(1)\ x_t(2)\ \cdots\ x_t(N_F\ )\ ,t = 1,2,...,T$ is obtained in each branch of the transmitter, where N_F is the size of the fast Fourier transform (FFT) and $x_t(n_f) \in \{0,S\},n_f = 1,2,...,N_F$.

INTERNATIONAL JOURNAL OF TECHNO-ENGINEERING
IJTE
ISSN: 2057-5688

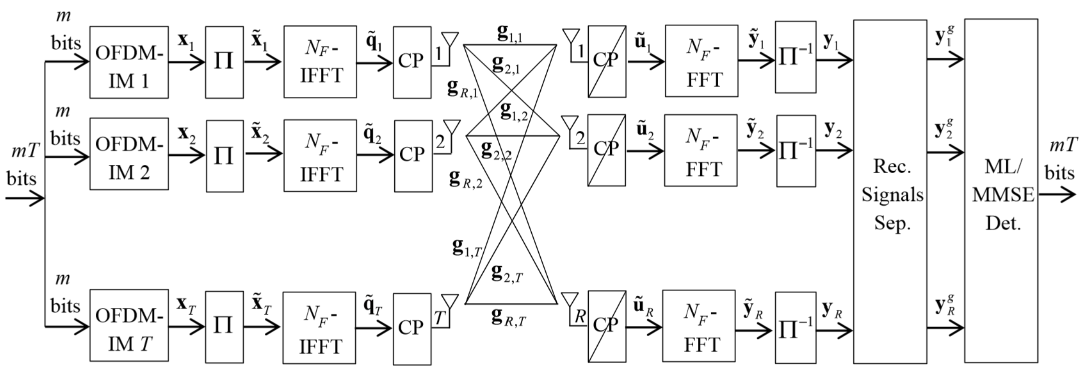

Fig. 1. Transceiver Structure of the MIMO-OFDM-IM Scheme for a $T \times R$ MIMO System

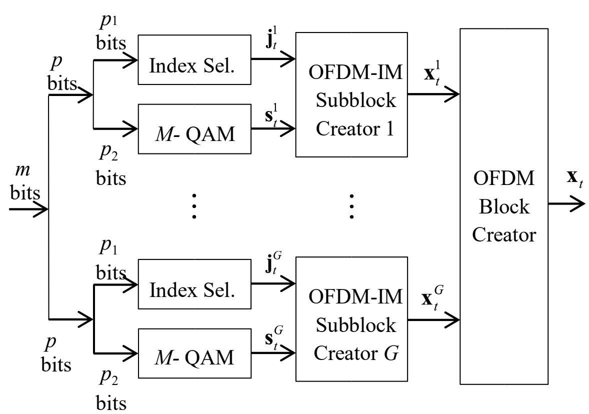

Fig. 2. OFDM index modulators at each brach of the transmitter

According to the OFDM-IM principle [10], which is carried out simultaneously in each branch of the transmitter, these m bits are split into G groups each containing $p = p_1 + p_2$ bits, which are used to form OFDM-IM subblocks $\mathbf{x}^g_t=[x_t (1)\ x_t (2) \cdots x_t (N)]1,2,...,G$ of length $N = N_F /G$, where $x^g_t (n) \in \{0,S\},n = 1,2,...,N$. At each subblock g, considering the corresponding $p_1 = \mathrm{b}\log_2 (C (N,K))\mathrm{c}$ bits, only K out of N available subcarriers are selected as active by the index selector, where the indices of the active subcarriers are denoted by $\mathbf{j}^g_t = {}^{\mathrm{h}}j_t^g(1)\ j_t^g(2) \cdots j_t^g(K)^{\mathrm{iT}}$, $j_t^g(k) \in \{1,\cdots ,N\}$, $k = 1,2,...,K$. On the other hand, the remaining $N - K$ subcarriers are inactive and set to zero. In the mean time, the remaining $p_2 = K \log_2(M)$ bits are mapped onto the considered M-ary quadrature(M-QAM) signal constellation to obtain $\mathbf{s}^g_t = \mathrm{h}sg_t\ (1)\ sg_t\ (2) \cdots sg_t\ (K)\mathrm{iT}$, amplitude modulation ($s^g_t\ (k) \in$ S, $k = 1,2,...,K$. For each OFDM-IM subblock $\mathbf{x}^g_t$, the K elements of $\mathbf{s}^g_t$ modulates

TABLE I

INTERNATIONAL JOURNAL OF TECHNO-ENGINEERING
IJTE

ISSN: 2057-5688

REFERENCE LOOK-UP TABLE FOR $N = 4, K = 2$ AND $p_1 = 2$

the K active subcarriers whose indices given by $\mathbf{j}^{g}_{t}$. Therefore, unlike classical MIMO-OFDM, $\mathbf{x}_t, t = 1,2,...,T$ contains some zero terms whose positions carry information for MIMOOFDM-IM[1].

Active subcarrier index selection is performed at OFDM index modulators of the transmitter by either using reference look-up tables for smaller values of active subcarriers (K) and subblock sizes (N) or an index selection procedure based on the combinatorial number theory for higher

values of K and N. An example look-up table of size $C = 2^{p1} = 4$ is given in Table I for $N = 4, K = 2$, where $p_1 = 2$ bits can be used to determine the indices of the two active

subcarriers out of four available subcarriers. For higher values of K and N, the combinatorial algorithm provides the selected indices according to the incoming p_1 bits [10].

In each branch of the transmitter, the OFDM index modulators construct the OFDM-IM subblocks first, then concatenate these G subblocks to obtain the main OFDM-IM blocks $\mathbf{x}_t, t = 1,2,...,T$. $G \times N$ block

Bits	*Indices* $(\mathbf{j}^{g}_{t})^T$	*OFDM-IM subblocks* $(\mathbf{x}^{g}_{t})^{\mathrm{T}}$
[0 0]	h i 1 3	h i gg $s_t(1)$ 0 $s_t(2)$ 0
[0 1]	h i 2 4	h i g g 0 $s_t(1)$ 0 $s_t(2)$
[1 0]	h i 1 4	h i gg $s_t(1)$ 0 0 $s_t(2)$
[1 1]	h i 2 3	h i g g 0 $s_t(1)$ $s_t(2)$ 0

interleavers (Π) are employed at the transmitter to transmit the elements of the subblocks from uncorrelated channels. Then, inverse FFT (IFFT) operators process the interleaved OFDM-IM frames $\tilde{\mathbf{x}}_t, t = 1,2,...,T$ and obtain $\tilde{\mathbf{q}}_t, t = 1,2,...,T$. It is assumed that the time-domain OFDM symbols are normalized to have unit energy, i.e., $E\left\{\tilde{\mathbf{q}}_t^{\mathrm{H}}\tilde{\mathbf{q}}_t\right\} = N_F$

for all t.

After the IFFT operation, a cyclic prefix (CP) of C_p samples is appended to the beginning of the OFDM-IM frames in each branch of the transmitter. After parallel-to-serial and digital-toanalog conversions, the resulting signals are sent simultaneously from T transmit antennas over a frequency-selective Rayleigh fading MIMO channel which can be represented by $\mathbf{g}_{r,t} \in \mathbb{C}^{L\times 1}$, where L is the

.

ISSN: 2057-5688

number of channel taps. We assume that the elements of $\mathbf{g}_{r,t}$ are independent

and identically distributed (iid) with CN$(0,1/L)$.

Based on the assumption that the wireless channels remain constant during the transmission of

a MIMO-OFDM-IM frame and $C_p > L$, after removing the CP and performing FFT

$$\left[(\mathbf{y}_r^1)^{\mathrm{T}} \cdots (\mathbf{y}_r^G)^{\mathrm{T}}\right]^{\mathrm{T}}, \mathbf{x}_t = \left[(\mathbf{x}_t^1)^{\mathrm{T}} \cdots (\mathbf{x}_t^G)^{\mathrm{T}}\right]$$

operations in each branch of the receiver, the input-output relationship of the MIMO-OFDM-IM scheme in

the frequency domain is obtained for $r = 1,2,...,R$ as follows:

$$\tilde{\mathbf{y}}_r = \sum_{t=1}^{T} \operatorname{diag}(\tilde{\mathbf{x}}_t)\, \mathbf{h}_{r,t} + \mathbf{w}_r.$$

In (1), $\tilde{\mathbf{y}}_r = [\tilde{y}_r(1)\ \tilde{y}_r(2) \cdots \tilde{y}_r(N_F)\ ]^{\mathrm{T}}$ is the vector of the received signals for receive antenna r, the frequency response of the wireless channel between the transmit antenna t and receive antenna r is denoted by $\mathbf{h}_{r,t} \in \mathbb{C}^{N_F\times 1}$, and $\mathbf{w}_r \in \mathbb{C}^{N_F\times 1}$ stands for the vector of noise samples. The elements of $\mathbf{h}_{r,t}$ and $\mathbf{w}_r$ follow CN $(0,1)$ and CN $(0,N_{0,F})$ distributions, respectively, where $N_{0,F}$ denotes the variance of the noise samples in the frequency domain, and it is related to the variance of the noise samples in the time domain as $N_{0,F} = (K/N)N_{0,T}$.

After deinterleaving operation, the received signals for receive antenna r are obtained as

$$\mathbf{y}^r = \sum_{t=1}^{T} \operatorname{diag}(\mathbf{x}_t)\breve{\mathbf{h}}_{r,t} + \breve{\mathbf{w}}_r$$

where $\breve{\mathbf{h}}_{r,t}$ and $\breve{\mathbf{w}}_r$ are deinterleaved versions of $\mathbf{h}_{r,t}$ and $\mathbf{w}_r$, respectively. As seen from Fig. 1, before the detection of the MIMO-OFDM-IM scheme, the received signals in (2) are separated

T

for each subblock $g = 1,2,...,G$ as $\mathbf{y}_r =$,

$\breve{\mathbf{h}}_{r,t} = [(\breve{\mathbf{h}}^1_{r,t})^{\mathrm{T}} \cdots (\breve{\mathbf{h}}^G_{r,t})^{\mathrm{T}}]^{\mathrm{T}}$, $\breve{\mathbf{w}}_r = \left[(\breve{\mathbf{w}}_r^1)^{\mathrm{T}} \cdots (\breve{\mathbf{w}}_r^G)^{\mathrm{T}}\right]^{\mathrm{T}}$. Then, we obtain the following signal model for each subblock g:

$$\mathbf{y}_r^g = \sum_{t=1}^{T} \operatorname{diag}(\mathbf{x}^g_t)\breve{\mathbf{h}}^g_{r,t} + \breve{\mathbf{w}}_r^g,$$

where $\mathbf{y}_r^g = [y_r^g(1)\ y_r^g(2) \cdots y_r^g(N)]^{\mathrm{T}}$ is the vector of the received signals at receive antenna r, $\mathbf{x}_t^g = \left[x_t^g(1)\ x_t^g(2) \cdots x_t^g(N)\right]^{\mathrm{T}}$ is the OFDM-IM subblock g for transmit antenna t

$\left[\breve{h}^g_{r,t}(1)\ \breve{h}^g_{r,t}(2) \cdots \breve{h}^g_{r,t}(N)\right]^{\mathrm{T}}$ and $\breve{\mathbf{w}}_r^g = \left[\breve{w}_r^g(1)\ \breve{w}_r^g(2) \cdots \breve{w}_r^g(N)\right]^{\mathrm{T}}$.

INTERNATIONAL JOURNAL OF TECHNO-ENGINEERING
IJTE
ISSN: 2057-5688

For the presentation and analysis of different type of detectors, the following signal model is

obtained from (3) for subcarrier n of subblock g:

$$\begin{bmatrix} y_1^g(n) \\ y_2^g(n) \\ \vdots \\ y_R^g(n) \end{bmatrix} = \begin{bmatrix} \breve{h}_{1,1}^g(n) & \cdots & \breve{h}_{1,T}^g(n) \\ \breve{h}_{2,1}^g(n) & \cdots & \breve{h}_{2,T}^g(n) \\ \vdots & \ddots & \vdots \\ \breve{h}_{R,1}^g(n) & \cdots & \breve{h}_{R,T}^g(n) \end{bmatrix} \begin{bmatrix} x_1^g(n) \\ x_2^g(n) \\ \vdots \\ x_T^g(n) \end{bmatrix} + \begin{bmatrix} \breve{w}_1^g(n \\ \breve{w}_2^g(n \\ \vdots \\ \breve{w}_R^g(n \end{bmatrix}$$

$$\bar{\mathbf{y}}_n^g = \mathbf{H}_n^g$$

for $n = 1,2,...,N$ and $g = 1,2,...,G$, where $\bar{\mathbf{y}}_n^g$ is the received signal vector, $\mathbf{H}^g_n \in \mathbb{C}^{R\times T}$ is the corresponding channel matrix which contains the channel coefficients between transmit and receive antennas and assumed to be perfectly known at the receiver, $\bar{\mathbf{x}}^g_n$ is the data vector which contains the simultaneously transmitted symbols from all transmit antennas and can have zero terms due to index selection in each branch of the transmitter and $\bar{\mathbf{w}}_n^g$ is the noise vector.

The signal-to-noise ratio (SNR) is defined as SNR = $E_b/N_{0,T}$ where $E_b = (N_F + C_p)/m$ [joules/bit] is the average transmitted energy per bit. The spectral efficiency of the MIMOOFDM-IM scheme is calculated as $mT/(N_F + C_p)$ [bits/s/Hz].

III. ML DETECTION OF MIMO-OFDM-IM

In this section, we propose ML and near-ML detectors of the MIMO-OFDM-IM scheme which can be used in applications where the BER is critical. We also derive the ABEP of the brute-force ML detector which can be considered as a performance benchmark for the near-ML

detector, whose theoretical performance analysis is intractable.

A. Brute-Force ML Detecion of MIMO-OFDM-IM

A straightforward solution to the detection problem of (3) is the use of ML detector which

can be realized for each subblock g as

$$(\mathbf{x}_1^g, \ldots, \mathbf{x}_T^g)_{\text{ML}} = \arg\min_{(\mathbf{x}_1^g,\ldots,\mathbf{x}_T^g)} \sum_{r=1}^{R} \left\| \mathbf{y}_r^g - \sum_{t=1}^{T} (\mathbf{x}_t^g)\, \breve{\mathbf{h}}_{r,t}^g \right\|^2$$

As seen from (5), the ML detector has to make a joint search over all transmit antennas due the interference between the subblocks of different transmit antennas.

In this subsection, the ABEP of MIMO-OFDM-IM is derived by the PEP calculation for MIMO-OFDM-IM subblocks. Since the pairwise error (PE) events within different subblocks are identical, it is sufficient to investigate the PE events within a single

ISSN: 2057-5688

subblock to determine the overall system performance.

Stacking the received signals in (4) for N consecutive subcarriers of a given subblock g, we

Obtain

$$\begin{bmatrix} \bar{\mathbf{y}}_1^g \\ \bar{\mathbf{y}}_2^g \\ \vdots \\ \bar{\mathbf{y}}_N^g \end{bmatrix} = \begin{bmatrix} \mathbf{H}_1^g & \mathbf{0} & \dots & \mathbf{0} \\ \mathbf{0} & \mathbf{H}_2^g & \dots & \mathbf{0} \\ \vdots & & \ddots & \vdots \\ \mathbf{0} & \mathbf{0} & \dots & \mathbf{H}_N^g \end{bmatrix} \begin{bmatrix} \bar{\mathbf{x}}_1^g \\ \bar{\mathbf{x}}_2^g \\ \vdots \\ \bar{\mathbf{x}}_N^g \end{bmatrix} + \begin{bmatrix} \bar{\mathbf{w}}_1^g \\ \bar{\mathbf{w}}_2^g \\ \vdots \\ \bar{\mathbf{w}}_N^g \end{bmatrix}$$

$$\mathbf{y}^g = \mathbf{H}^g \mathbf{x}^g + \mathbf{w}^g$$

where $\mathbf{0}$ denotes the all-zero matrix with dimensions $R\times T$, $\mathbf{y}^g \in \mathbb{C}^{RN\times 1}$ is the vector of

$$P\left(\mathbf{x}^g \rightarrow \mathbf{e}^g \mid \mathbf{H}^g\right) = Q\left(\sqrt{\frac{\left\|\mathbf{H}^g\left(\mathbf{x}^g - \mathbf{e}^g\right)\right\|^2}{2N_{0,F}}}\right)$$

stacked received signals for the corresponding subblock, $\mathbf{H}^g \in \mathbb{C}^{RN\times TN}$ is the block-diagonal channel matrix, $\mathbf{x}^g \in \mathbb{C}^{TN\times 1}$ is the equivalent data vector which has $(CM^K)^T$ possible realizations according to index modulation and $\mathbf{w}^g \in \mathbb{C}^{RN\times 1}$ is the noise vector. Using the matrix form given in (6), the ML detection of MIMO-OFDM-IM for each subblock g can also be performed as $(\mathbf{x}^g)_{\mathrm{ML}} =$

$${}^g = \left[(\bar{\mathbf{e}}_1^g)^{\mathrm{T}}\ (\bar{\mathbf{e}}_2^g)^{\mathrm{T}}\ \cdots\ (\bar{\mathbf{e}}_N^g)^{\mathrm{T}}\right]$$

$$\arg\min_{\mathbf{x}^g} \left\|\mathbf{y}^g - \mathbf{H}^g\mathbf{x}^g\right\|^2. \qquad (7)$$

Considering the signal model of (6), for a given channel matrix $\mathbf{H}^g$, if $\mathbf{x}^g$ is transmitted and it is

T

erroneously detected as $\mathbf{e}^g$, where $\mathbf{e}$, the conditional PEP (CPEP)

can be calculated as

$$P\left(\mathbf{x}^g \rightarrow \mathbf{e}^g \mid \mathbf{H}^g\right) = P\left(\left\|\mathbf{y}^g - \mathbf{H}^g\mathbf{x}^g\right\|^2 >$$

After some algebra, the CPEP of the MIMO-

$$M_\Gamma(t) = \prod_{n=1}^{N}\left[\det\left(\mathbf{I}_T - t\mathbf{L}\mathbf{Q}_n^g\right)\right]^{-R} = \prod_{n=1}^{N}\left(1 - t\left\|\bar{\mathbf{x}}_n^g - \bar{\mathbf{e}}_n^g\right\|^2\right)$$

OFDM-IM scheme is obtained as

$$\begin{aligned} &P\left(\mathbf{x}^g \rightarrow \mathbf{e}^g \mid \mathbf{H}^g\right) \\ &= P\left(\left\|\mathbf{H}^g\mathbf{x}^g\right\|^2 - \left\|\mathbf{H}^g\mathbf{e}^g\right\|^2 - 2\Re\left\{(\mathbf{y}^g)^{\mathrm{H}}\mathbf{H}\right.\right. \\ &= P\left(-\left\|\mathbf{H}^g\left(\mathbf{x}^g - \mathbf{e}^g\right)\right\|^2 - 2\Re\left\{(\mathbf{w}^g)^{\mathrm{H}}\mathbf{H}\right.\right. \\ &= P\left(D > 0\right) \end{aligned}$$

where $D \sim \mathcal{N}(m_D, \sigma_D^2)$ with $m_D = -\left\|\mathbf{H}^g\left(\mathbf{x}^g - \mathbf{e}^g\right)\right\|^2$ and $\sigma_D^2 = 2N_{0,F}\left\|\mathbf{H}^g\left(\mathbf{x}^g - \mathbf{e}^g\right)\right\|^2$, for which we obtain

Using the alternative form of the Q-function [24], (10) can be rewritten as

$$P\left(\mathbf{x}^g \rightarrow \mathbf{e}^g \mid \mathbf{H}^g\right) = \frac{1}{\pi}\int_0^{\pi/2} \exp\left(-\frac{\left\|\mathbf{H}^g\left(\mathbf{x}^g\right.\right.}{4N_{0,F}}\right.$$

Integrating the CPEP in (11) over the probability density function (pdf) of $\Gamma =$

,

the unconditional PEP (UPEP) of the MIMO-OFDM-IM scheme is obtained as

INTERNATIONAL JOURNAL OF TECHNO-ENGINEERING
IJTE
ISSN: 2057-5688

$$P\left(\mathbf{x}^g \rightarrow \mathbf{e}^g\right)=\frac{1}{\pi} \int_0^{\pi/2}$$

where $M_\Gamma(t)$ is the moment generating function (mgf) of Γ. Expressing Γ in quadratic form as

$$\Gamma=\sum_{n=1}^{N}\left\|\mathrm{H}_n^g\left(\bar{\mathrm{x}}_n^g-\bar{\mathrm{e}}_n^g\right)\right\|^2=\sum_{n=1}^{N}\sum_{r=1}^{R}\left(\mathrm{H}_n^g\right)_{r*}\mathrm{Q}_n^g\left(\mathrm{H}_n^g\right)$$

where $\mathbf{Q}^g_n = (\bar{\mathbf{x}}^g_n - \bar{\mathbf{e}}^g_n)(\bar{\mathbf{x}}^g_n - \bar{\mathbf{e}}^g_n)^{\mathrm{H}}$. According to the quadratic form of Γ given in (13), its mgf is

$-R$

obtained as [25]since $(\mathbf{H}^g_n)_{r*}$'s are i.i.d. for all r and n, $\mathbf{L}=E\left\{\left(\mathbf{H}_n^g\right)_{r*}^{\mathrm{H}}\left(\mathbf{H}_n^g\right)_{r*}\right\}=\mathbf{I}_T$ and rank$(\mathbf{Q}^g_n) = 1$. Finally, from (12),

On the other hand, the distance spectrum of the MIMO-OFDM-IM is improved due to the PE events in which there are errors in active indices since these PE events have lower occurrence probabilities.

Remark 2: After the evaluation of the UPEP, the ABEP of the MIMO-OFDM-IM scheme can be obtained by the asymptotically tight union upper bound as

$$P_b \leq \frac{1}{n_b n(\mathbf{x}^g)} \sum_{\mathbf{x}^g} \sum_{\mathbf{e}^g}$$

where $n_b = pT$ is the total number of information bits carried by $\mathbf{x}^g$, $n(\mathbf{x}^g) = (CM^K)^T$ is

the UPEP of the MIMO-OFDM-IM scheme is obtained as

$$P\left(\mathbf{x}^g \rightarrow \mathbf{e}^g\right)=\frac{1}{\pi} \int_0^{\pi/2} \prod_{n=1}^{N}\left(\frac{\mathrm{si}}{\sin^2\theta +}\right.$$

Please note that the integral given in (14) has closed form solutions in Appendix 5A of [24] for different N values.

Remark 1: For the worst case PE events in which there are no active indices errors and a single M-ary symbol is erroneously detected in $\mathbf{e}^g$, we obtain $\left\|\bar{\mathbf{x}}_n^g-\bar{\mathbf{e}}_n^g\right\|^2 \neq 0$ for only a single n value. In this case, the diversity order of the MIMO-OFDM-IM scheme is calculated after some manipulation as [26]

$$G_d=-\lim_{N_{0,F}\rightarrow 0}\frac{\log\left(P\left(\mathbf{x}^g \rightarrow\right.\right.}{\log\left(1/N_{0,\right.}}$$

the total number of possible realizations of $\mathbf{x}^g$ and $n(\mathbf{x}^g, \mathbf{e}^g)$ is the number of bit errors for the corresponding PE event $(\mathbf{x}^g \rightarrow \mathbf{e}^g)$.

B. Simplified Near-ML Detection of MIMO-OFDM-IM

The total decoding complexity of the brute-force ML detector given in (5) and (7) in terms of complex multiplications (CMs) is $\sim$ O(M^{KT}), which is considerably higher than that of classical MIMO-OFDM, whose complexity is $\sim$ O(M^T), even if assuming that both schemes use the

INTERNATIONAL JOURNAL OF TECHNO-ENGINEERING
IJTE

ISSN: 2057-5688

same constellation order. In this section, we propose a near-ML detector for the MIMO-OFDMIM scheme which has the same order decoding complexity compared to classical MIMO-OFDM ML detector.

The ML detector in (5) maximizes the joint conditional pdf of $p\left(\mathbf{y}_1^g, \ldots, \mathbf{y}_R^g \mid \mathbf{x}_1^g, \ldots, \mathbf{x}_T^g\right)$, i.e., jointly searches for $\mathbf{x}_1^g, \ldots, \mathbf{x}_T^g$ using the reference look-up table. On the other hand, the proposed near-ML detector calculates a probabilistic measure for each element ($\mathbf{x}^g_t$) of the reference look-up table for a given transmit antenna; therefore, it reduces the size of the search space considerably. For this purpose, the near-ML detector considers the model in (4) and implements the following steps:[2]

1) Calculate $N(M+1)^T$ different conditional probability values of $P(\bar{\mathbf{x}}^g_n | \bar{\mathbf{y}}^g_n)$ by considering

$$P\left(\bar{\mathbf{x}}_n^g \mid \bar{\mathbf{y}}_n^g\right) = \frac{f\left(\bar{\mathbf{y}}_n^g \mid \bar{\mathbf{x}}_n^g\right) P\left(\bar{\mathbf{x}}_n^g\right)}{f\left(\bar{\mathbf{y}}_n^g\right)} = \frac{f\left(\bar{\mathbf{y}}_n^g \mid \bar{\mathbf{x}}_n^g\right) P\left(\bar{\mathbf{x}}_n^g\right)}{\sum f\left(\bar{\mathbf{y}}_n^g \mid \bar{\mathbf{x}}_n^g\right) P\left(\bar{\mathbf{x}}\right.} \quad (17)$$

$\bar{\mathbf{x}}^g_n$

for $n = 1,\ldots,N$ and all possible $\bar{\mathbf{x}}^g_n$ vectors where conditioned on $\bar{\mathbf{x}}^g_n$, $\bar{\mathbf{y}}^g_n$ has the multivari-ate complex Gaussian distribution with pdf.

$$f\left(\bar{\mathbf{y}}_n^g \mid \bar{\mathbf{x}}_n^g\right) = \left(\pi N_{0,F}\right)^{-R} \exp\left(-\frac{\left\|\bar{\mathbf{y}}_n - \mathbf{H}_n \bar{\mathbf{x}}_n\right\|^2}{N_{0,F}}\right)$$

2) In order to obtain the occurrence probability for each element ($\mathbf{x}^g_t$) of the reference look-up table, calculate

$$P\left(\mathbf{x}_t^g\right) = \prod_{n=1}^{N} P\left(x_t^g(n)\right) = \prod_{n=1}^{N} \sum_{\bar{\mathbf{x}}_n^g, \bar{x}_n^g(t) = x_t^g(n)} P\left(\bar{\mathbf{x}}_n^g \mid \bar{\mathbf{y}}_n^g\right) \quad (18)$$

where $\bar{x}^g_n(t)$ is tth element of $\bar{\mathbf{x}}^g_n \in \mathbb{C}^{T\times 1}$. (18) provides a clever way to transform the probabilities of $P(\bar{\mathbf{x}}^g_n | \bar{\mathbf{y}}^g_n)$, which consider the symbols transmitted from different antennas, into the probabilities of $P(\mathbf{x}^g_t)$, which are distinct for each transmit antenna.

3) Finally, after the calculation of CM^K probability values for each transmit antenna t, decide on the most likely element of the reference look-up table as

$$\left(\mathbf{x}_t^g\right)_{\text{near-ML}} = \arg\max_{\mathbf{x}_t^g} P$$

As seen from (17)-(18), for the calculation of $P(\mathbf{x}^g_t)$ values, a search over the possible realizations of $\bar{\mathbf{x}}^g_n$ has to be made, which reduces the size of the search space to $(M+1)^T$ for each n value since $\bar{x}^g_n(t) \in \{0,\mathcal{S}\}$ and a total of $\sim O(M^T)$ CMs are required. The

.

following numerical example shows the

steps of the near-ML detector.
Example 1: Consider the MIMO-OFDM-IM scheme with the following system parameters: $T = M = K = 2$, $N = 4$. For these values, the reference look-up table contains $CM^K = 16$ elements.

In this case, $(\bar{\mathbf{x}}_n^g)^{\mathrm{T}}$ has $(M+1)^T = 9$ possible realizations: $\begin{bmatrix}0 & 0\end{bmatrix}$, $\begin{bmatrix}0 & 1\end{bmatrix}$, $\begin{bmatrix}0 & -1\end{bmatrix}$, $\begin{bmatrix}1 & 0\end{bmatrix}$, $\begin{bmatrix}1 & 1\end{bmatrix}$, $\begin{bmatrix}1 & -1\end{bmatrix}$, $\begin{bmatrix}-1 & 0\end{bmatrix}$, $\begin{bmatrix}-1 & 1\end{bmatrix}$ and $\begin{bmatrix}-1 & -1\end{bmatrix}$, with the following probabilities: 0.25,0.125,0.125,0.125,0.0625,0.0625,0.125, 0.0625 and 0.0625, respectively.

First, the near-ML detector calculates and stores the probabilities $P(\bar{\mathbf{x}}_n^g \mid \bar{\mathbf{y}}_n^g)$ using the received signals $\bar{\mathbf{y}}_n^g$ and possible $\bar{\mathbf{x}}_n^g$ vectors for $n = 1,2,3,4$, where a total of $N(M+1)^T = 36$ probability

calculations are required. As an example, for $n = 1$, nine probability values of $P(\bar{\mathbf{x}}_1^g \mid \bar{\mathbf{y}}_1^g)$ are calculated and stored using (17).

Second, the occurrence probability of the each element of the reference look-up table is calculated from (18). Let us consider that we want to calculate the probability of $P(\mathbf{x}_1^g = \begin{bmatrix}1 & 0 & -1 & 0\end{bmatrix}^{\mathrm{T}})$, where $\begin{bmatrix}1 & 0 & -1 & 0\end{bmatrix}^{\mathrm{T}}$ is selected from the look-up table (Table I). According to (18), we have

$$P(\mathbf{x}_1^g = \begin{bmatrix}1 & 0 & -1 & 0\end{bmatrix}$$

$$= P(x^g{}_1(1) = 1)P(x^g{}_1(2) = 0)P(x^g{}_1(3) = -1)P(x^g{}_1(4) = 0)$$

where

$$P(x_1^g(1) = 1) = \sum_{\bar{\mathbf{x}}_1^g, \bar{x}_1^g(1)=1} P(\bar{\mathbf{x}}_1^g \mid \bar{\mathbf{y}}_1^g) = P\left(\bar{\mathbf{x}}_1^g = \begin{bmatrix}1 & 0\end{bmatrix}^{\mathrm{T}} \mid \bar{\mathbf{y}}_1^g\right)$$
$$+ P\left(\bar{\mathbf{x}}_1^g = \begin{bmatrix}1 & 1\end{bmatrix}^{\mathrm{T}} \mid \bar{\mathbf{y}}_1^g\right) + P\left(\bar{\mathbf{x}}_1^g = \begin{bmatrix}1 & -1\end{bmatrix}^{\mathrm{T}} \mid \bar{\mathbf{y}}_1^g\right),$$
$$P(x_1^g(2) = 0) = \sum_{\bar{\mathbf{x}}_2^g, \bar{x}_2^g(1)=0} P(\bar{\mathbf{x}}_2^g \mid \bar{\mathbf{y}}_2^g) = P\left(\bar{\mathbf{x}}_2^g = \begin{bmatrix}0 & 0\end{bmatrix}^{\mathrm{T}} \mid \bar{\mathbf{y}}_2^g\right)$$
$$+ P\left(\bar{\mathbf{x}}_2^g = \begin{bmatrix}0 & 1\end{bmatrix}^{\mathrm{T}} \mid \bar{\mathbf{y}}_2^g\right) + P\left(\bar{\mathbf{x}}_2^g = \begin{bmatrix}0 & -1\end{bmatrix}^{\mathrm{T}} \mid \bar{\mathbf{y}}_2^g\right),$$
$$P(x_1^g(3) = -1) = \sum_{\bar{\mathbf{x}}_3^g, \bar{x}_3^g(1)=-1} P(\bar{\mathbf{x}}_3^g \mid \bar{\mathbf{y}}_3^g) = P\left(\bar{\mathbf{x}}_3^g = \begin{bmatrix}-1 & 0\end{bmatrix}^{\mathrm{T}} \mid \bar{\mathbf{y}}_3^g\right)$$

$$+P\left(\bar{\mathbf{x}}_3^g=\begin{bmatrix}-1 & 1\end{bmatrix}^{\mathrm{T}}|\,\bar{\mathbf{y}}_3^g\right)+P\left(\bar{\mathbf{x}}_3^g=\begin{bmatrix}-1 & -1\end{bmatrix}^{\mathrm{T}}|\,\bar{\mathbf{y}}_3^g\right),$$

$$P(x_1^g(4)=0)=\sum_{\mathbf{x}^{-g}_4,\bar{x}_4^g(1)=0}P\left(\bar{\mathbf{x}}_4^g\,|\,\bar{\mathbf{y}}_4^g\right)=P\left(\bar{\mathbf{x}}_4^g=\begin{bmatrix}0 & 0\end{bmatrix}^{\mathrm{T}}|\,\bar{\mathbf{y}}_4^g\right)$$

$$+P\left(\bar{\mathbf{x}}_4^g=\begin{bmatrix}0 & 1\end{bmatrix}^{\mathrm{T}}|\,\bar{\mathbf{y}}_4^g\right)+P\left(\bar{\mathbf{x}}_4^g=\begin{bmatrix}0 & -1\end{bmatrix}^{\mathrm{T}}|\,\bar{\mathbf{y}}_4^g\right).$$

$P(\mathbf{x}_2^g = \begin{bmatrix}1 & 0 & -1 & 0\end{bmatrix}$ Similarly,) can be calculated considering the second elements of $\mathbf{x}^{-g}{}_n$.

Finally, the most likely element of the look-up table is determined from (19) after the calculation of CM^K probability values, where $^{\mathrm{P}}{}_{\mathbf{x}}gt\ P(\mathbf{x}^g{}_t) = 1$.

IV. MMSE DETECTION OF MIMO-OFDM-IM SCHEME

The total decoding complexity of the brute-force and near-ML detectors can be considerably high for higher order modulations and MIMO systems. In this section, instead of the exponentially increasing decoding complexity of the ML detectors, we deal with the MMSE detection of the MIMO-OFDM-IM scheme, which significantly reduces the decoding complexity. The approximate ABEP of the newly proposed simple MMSE detector is also provided which can be considered as a reference for MMSE and LLR detector.

A. Simple MMSE Detection of MIMO-OFDM-IM

Let us reconsider the following signal model which is obtained from (3) for subcarrier n of

subblock g:

$${}^g_t = \begin{bmatrix}z_1^g(t) & z_2^g(t) & \cdots & z_N^g(t)\end{bmatrix}$$

for $n = 1,2,...,N$ and $g = 1,2,...,G$. For classical MIMO-OFDM, the data symbols can be simply recovered after processing the received signal vector in (20) with the MMSE detector. On the other hand, due to the index information carried by the subblocks of the proposed scheme, it is not possible to detect the transmitted symbols by only processing $\mathbf{y}^{-}{}_n{}^g$ for a given subcarrier n in the MIMO-OFDM-IM scheme. Therefore, N independent and successive

MMSE detections are performed for the proposed scheme using the MMSE filtering matrix

[27] $\mathbf{W}_n^g=\left((\mathbf{H}_n^g)^{\mathrm{H}}\mathbf{H}_n^g+\frac{\mathbf{I}_T}{\rho}\right)^{-1}(\mathbf{H}_n^g)^{\mathrm{H}}$ for $n = 1,2,...,N$, where $\rho = \sigma_x 2/N0,F$, $\sigma x2 = K/N$ and $E\left\{\bar{\mathbf{x}}_n^g(\bar{\mathbf{x}}_n^g)^{\mathrm{H}}\right\}=\sigma_x^2\mathbf{I}_T$ due to zero terms in $\mathbf{x}^{-g}{}_n$ come from index selection. By the left

INTERNATIONAL JOURNAL OF TECHNO-ENGINEERING
IJTE
ISSN: 2057-5688

multiplication of $\bar{\mathbf{y}}_n^g$ given in (20) with $\mathbf{W}_n^g$, MMSE detection is performed as

$$\mathbf{z}_n^g = \mathbf{W}_n^g \bar{\mathbf{y}}_n^g = \mathbf{W}_n^g \mathbf{H}_n^g \bar{\mathbf{x}}_n^g + \mathbf{W}_n^g \bar{\mathbf{w}}_n^g$$

where $\mathbf{z}^g =$ $z_n^g(1)\ z_n^g(2) \cdots z_n^g(T)$ is the MMSE estimate of $\bar{\mathbf{x}}_n^g$. The MMSE estimate of MIMO-OFDM-IM subblocks $\hat{\mathbf{x}}_t^g = \mathrm{h}\hat{x}_t^g(1)\ \hat{x}_t^g(2) \cdots \hat{x}_t^g(N)\mathrm{i}^{\mathrm{T}}$ can be obtained by rearranging

the elements of $\mathbf{z}_n^g, n = 1,2,\ldots,N$ as $\hat{\mathbf{x}}$

$g = 1,2,\ldots,G$.

After MMSE filtering and rearranging the elements of MMSE filtered signals, the interference between the subblocks of different transmit antennas is eliminated and the transmitted subblocks

can be determined by considering the conditional multivariate pdf of $\hat{\mathbf{x}}_t^g$ given as [28]

$$f\left(\hat{\mathbf{x}}_t^g \mid \mathbf{x}_t^g\right) = \frac{\pi^{-N}}{\det(\mathbf{C})} \exp\Big(-$$

where considering that N-successive MMSE operations are independent, the conditional mean

and covariance matrix of $\hat{\mathbf{x}}_t^g$ conditioned on $\mathbf{x}_t^g$ are calculated respectively as

$$P\left(\mathbf{x}_t^g \rightarrow \mathbf{e}_t^g \mid \mathbf{H}_1^g, \cdots, \mathbf{H}_N^g\right)$$

$$\mathbf{m} = E\left\{\hat{\mathbf{x}}_t^g\right\} = \left[Q_1 x_t^g(1) \cdots Q_N x_t^g(N)\right]^{\mathrm{T}}$$
$$\mathbf{C} = \operatorname{cov}\left(\hat{\mathbf{x}}_t^g\right) = \operatorname{diag}\left(\left[C_1 \cdots C_N\right]\right). \quad (23)$$

For notational simplicity we defined Q_n, $(\mathbf{W}_n^g \mathbf{H}_n^g)_{t,t}, C_n$, $(\operatorname{cov}(\mathbf{z}_n^g))_{t,t}$ for $n = 1,2\ldots,N$ in (23). The statistics of $\hat{\mathbf{x}}_t^g$ are obtained from the conditional statistics of $\mathbf{z}_n^g$ conditioned

on

$x_t^g(n) \in \{0,\mathrm{S}\}$, which are given in [22] as

$$E\left\{\mathbf{z}_n^g\right\} = \mathbf{W}_n^g \mathbf{H}_n^g E\left\{\bar{\mathbf{x}}_n^g\right\} = \left(\mathbf{W}_n^g \mathbf{H}_n^g\right)_{*t} x_t^g(n)$$
$$\operatorname{cov}(\mathbf{z}_n^g) = \mathbf{W}_n^g \mathbf{H}_n^g \operatorname{cov}\left(\bar{\mathbf{x}}_n^g\right)\left(\mathbf{H}_n^g\right)^{\mathrm{H}}\left(\mathbf{W}_n^g\right)^{\mathrm{H}} + N_{0,F} \mathbf{W}_n^g \left(\mathbf{W}_n^g\right)^{\mathrm{H}} \quad (24)$$

where $\operatorname{cov}(\bar{\mathbf{x}}_n^g) =$ $\operatorname{diag}\left(\left[\sigma_x^2 \ \ldots \ \sigma_x^2 \ 0 \ \sigma_x^2 \ \ldots \ \sigma_x^2\right]\right)$ is a diagonal matrix whose tth diagonal element is zero.

The simple MMSE detector decides onto the most likely subblock by maximizing the conditional pdf of $\hat{\mathbf{x}}_t^g$ as

$$\left(\mathbf{x}_t^g\right)_{\mathrm{MMSE}} = \arg\max_{\mathbf{x}_t^g} f\left(\hat{\mathbf{x}}_t^g \mid \mathbf{x}_t^g\right) = \arg\min_{\mathbf{x}_t^g} \sum_{n=1}^{N} \frac{\left|\hat{x}_t^g(n) - Q_n x_t^g(n)\right|^2}{C_n} \quad (25)$$

where (25) is obtained by dropping the constant terms and considering the diagonal structure of $\mathbf{C}$. The CPEP of erroneously deciding in favor of $\mathbf{e}_t^g = {}^{\mathrm{h}}e_t^g(1)\ e_t^g(2) \cdots e_t^g(N)^{\mathrm{iT}}$ given that $\mathbf{x}_t^g$

is transmitted can be calculated as

INTERNATIONAL JOURNAL OF TECHNO-ENGINEERING
IJTE
ISSN: 2057-5688

$$= P\left(\sum_{n=1}^{N} \frac{|\hat{x}_t^g(n) - Q_n x_t^g(n)|^2 - |\hat{x}_t^g(n) - Q_n e_t^g(n)|^2}{C_n} > 0\right)$$

$$= P\left(\sum_{n=1}^{N} \left(Q_n^2\left(|x_t^g(n)|^2 - |e_t^g(n)|^2\right) - 2\Re\left\{Q_n \hat{x}_t^g(n)\left(x_t^g(n) - e_t^g(n)\right)^*\right\}\right)/C_n > 0\right) = P\left(D > 0\right) \tag{26}$$

where $D \sim N(m_D, \sigma_D^2)$ and considering $E\{\hat{x}^g_t(n)\} = Q_n x^g_t(n)$, $Var(\hat{x}^g_t(n)) = C_n$, and $Var(\Re\{\hat{x}^g_t(n)\}) = Var(\Im\{\hat{x}^g_t(n)\}) = C_n/2$ for complex M-QAM constellation symbols with i.i.d. real and imaginary parts, we obtain $m_D = -\sum_{n=1}^{N} V_n\Delta_n, \sigma_D^2 = 2\sum_{n=1}^{N} V_n\Delta_n$ which yields the following CPEP

$$P\left(\mathbf{x}_t^g \to \mathbf{e}_t^g \mid \mathbf{H}_1^g, \cdots, \mathbf{H}_N^g\right) = Q\left(\sqrt{\sum_{n=1}^{N} V_n\Delta_n}\right) \tag{27}$$

where $V_n \triangleq \frac{Q_n^2}{2C_n}$ and Δ_n , $|x^g_t(n) - e^g_t(n)|^2$. The r.v. V_n, which is the ratio of two correlated r.v.'s, has a nonparametric pdf which is a function of the SNR and is the same for all n and t.

Therefore, we provide an upper bound for the UPEP as follows.

Assuming $Q^2_n \approx 1$ and $C_n \approx N_{0,F}\left((\mathbf{H}_n^g)^{-1}((\mathbf{H}_n^g)^{-1})^{\mathrm{H}}\right)_{t,t}$ for $N_{0,F} \ll 1$, which is quite reasonable for practical applications, and using alternative form of the Q-function, we obtain

$$P\left(\mathbf{x}_t^g \to \mathbf{e}_t^g \mid \mathbf{H}_1^g, \cdots, \mathbf{H}_N^g\right) < \frac{1}{\pi}\int_0^{\pi/2} \exp\left(-\frac{\sum_{n=1}^{N} Z_n\Delta_n}{4N_{0,F}\sin^2\theta}\right) d\theta \tag{28}$$

where Z_n , $1/\left(\left[(\mathbf{H}_n^g)^{\mathrm{H}}\mathbf{H}_n^g\right]^{-1}\right)_{t,t}$ and the inequality arises from $V_n \approx Z_n/(2N_{0,F}) < V_n$. Considering that Z_n is exponentially distributed for $T = R$ [27] with mgf $M_{Z_n}(t) = 1/(1 - t)$ and for all n and t, integrating (28) over the pdf's of $Z_n, n = 1,2,\ldots,N$, the UPEP of the simple MMSE detector is obtained as

$$\begin{aligned} P\left(\mathbf{x}_t^g \to \mathbf{e}_t^g\right) &< \frac{1}{\pi}\int_0^{\pi/2} \prod_{n=1}^{N} M_{Z_n}\left(\frac{-\Delta_n}{4N_{0,F}\sin^2\theta}\right) d\theta \\ &= \frac{1}{\pi}\int_0^{\pi/2} \prod_{n=1}^{N} \left(\frac{\sin^2\theta}{\sin^2\theta + \frac{\Delta_n}{4N_{0,F}}}\right) d\theta \end{aligned} \tag{29}$$

which has a closed form solution in Appendix 5A of [24].

Remark 1: The diversity order of the simple MMSE detector is equal to one considering the worst case PE events in (29). The UPEP in (29) is independent of the number of

ISSN: 2057-5688

transmit antennas while $T = R$, and can be considered as an error performance upper bound for the MIMO-OFDM-IM scheme.

Remark 2: To obtain a tighter UPEP approximation, the averaging over V_n can be performed with a semi-analytical approach as follows. Considering the worst case PE events only in (27),

where Δ_n 6= 0 for a single $n \in \{1,2,...,N\}$ value, we obtain

$$P\left(\mathbf{x}_t^g \rightarrow \mathbf{e}_t^g \,|\, \mathbf{H}_1^g, \cdots ,\right.$$

For each SNR value, generating and storing $S = 10^6$ samples of V_n as $V_n(s), s = 1,2,...,S$ (as an example for $n = t = 1$ since the distribution of V_n is the same for all n and t), the UPEP of

the MIMO-OFDM-IM scheme can be obtained as

$$P\left(\mathbf{x}_t^g \rightarrow \mathbf{e}_t^g\right) \approx \frac{1}{S}\sum$$

Remark 3: After the evaluation of the UPEP, ABEP of the simple MMSE detector can be obtained

as

$$P_b \sim \frac{1}{pn(\mathbf{x}_t^g)} \sum\nolimits_{\mathbf{x}_t^g} \sum\nolimits_{\mathbf{e}}$$

where p is the total number of information bits carried by $\mathbf{x}^g{}_t$, $n(\mathbf{x}^g{}_t) = CM^K$ is the total number of possible realizations of $\mathbf{x}^g{}_t$ and $n(\mathbf{x}^g{}_t, \mathbf{e}^g{}_t)$ is the number of bit errors for the corresponding PE

event.

B. MMSE and LLR Detection of MIMO-OFDM-IM

MMSE and LLR detector of the MIMO-OFDM-IM scheme is proposed in [22] to implement a low complexity MMSE detection. Considering the conditional statistics of $x\hat{}^g{}_t(n)$, the MMSE and LLR detector of the MIMO-OFDM-IM scheme calculates the following LLR value for the nth subcarrier of tth transmitter for subblock g as

$$\lambda_t^g(n) = \ln\left(\sum_{m=1}^{M} \exp\left(-\frac{|\hat{x}_t^g(n) - Q_n s_m|^2}{C_n}\right.\right.$$

for $n = 1,2,...,N$, $t = 1,2,...,T$ and $g = 1,2,...,G$, where $s_m \in$ S. For the case of

reference look-up tables, the MMSE-LLR detector calculates LLR sums for each element of the look-up table and determines the active indices which provide the highest LLR sum. Details of this method can be found in [22].

In case of the selection of active indices with combinatorial algorithm, after the calculation of N LLR values form (33) for each subblock, the detector decides on K active indices out of them having maximum LLR values. Denoting the indices of these subcarriers by $\hat{\mathbf{j}}^g{}_t = [\hat{j}_t^g(1)\ \hat{j}_t^g(2) \cdots \hat{j}_t^g(K)]^{\mathrm{T}}$, the corresponding index selecting bits can be

INTERNATIONAL JOURNAL OF TECHNO-ENGINEERING
IJTE
ISSN: 2057-5688

determined with demapping algorithm, and the M-ary symbols transmitted by the active subcarriers are

determined for $k = 1,2,...,K$ as

$$(s_t^g(k))_{\text{MMSE}} = \arg\min_{s_m \in \mathcal{S}} \left| \hat{x}_t^g(\hat{j}_t^g(k)) - Q_{\hat{j}_t^g(k)} s_m \right|^2 \quad (34)$$

C. MMSE and LLR Detection of MIMO-OFDM-IM with OSIC

Successive interference cancellation (SIC) techniques have been efficiently implemented for MMSE detection based V-BLAST systems to obtain better BER performance with the price of increased decoding complexity [29]. In other words, MMSE with SIC is an intermediate solution between ML and classical MMSE detections and provides a trade-off in performance and complexity. In this subsection, a novel OSIC based sequential MMSE-LLR detector is proposed for the MIMO-OFDM-IM scheme to further improve the error performance.

The OSIC-MMSE-LLR detector of the MIMO-OFDM-IM scheme considers N successive MMSE detections and obtains the following empirical min-max metric for each subblock g of

each transmit antenna $t, t = 1,2,...,T$ as

$$\gamma_t = \max\left\{ \left\| \left((\mathbf{G}_1^g)^+ \right)_{t*} \right\|^2 \right.$$

where Q_n is defined in (23). The above process is repeated for each subblock of each transmit antenna. As seen from (33)-(34), the complexity of the MMSE-LLR detector, in terms of CMs, is ∼ O(M) per subcarrier.

Where

$$\mathbf{G}_n^g = \begin{bmatrix} \mathbf{H}_n^g \\ (1/\sqrt{\rho})\mathbf{I}_T \end{bmatrix}, \text{ and } (\mathbf{G}_n^g)^+ = \left((\mathbf{G}_n^g)^{\mathrm{H}} \mathbf{G}_n^g \right)^{-1} (\mathbf{G}_n^g)^{\mathrm{H}}$$

.The subblock of the transmit

antenna with the minimum metric (γ_t) is selected as the best subblock in terms of signal-tointerference-plus-noise ratio (SINR) and ordering is performed according to $\gamma_t, t = 1,2,...,T$. For each transmit antenna, the MMSE estimate of MIMO-OFDM-IM subblocks are obtained as $\hat{x}^g_t(n) = \mathbf{q}^g_{n,t}\bar{\mathbf{y}}^g_n$, where $\mathbf{q}^g_{n,t}$, $(\mathbf{W}_n^g)_{t*} \in \mathbb{C}^{1\times R}$ for $n = 1,2,...,N$. The conditional mean and

variance ($\tilde{C}_n$) of Gaussian distributed $\hat{x}^g_t(n)$ is calculated for this case respectively as

$$E\left\{\hat{x}_t^g(n)\right\} = \left(\mathbf{q}_{n,t}^g \mathbf{H}_n^g\right)_{*t} x_t^g(n) = \tilde{Q}_n x_t^g(n)$$

$$Var\left(\hat{x}_t^g(n)\right) = \mathbf{q}_{n,t}^g \mathbf{H}_n^g \operatorname{cov}\left(\bar{\mathbf{x}}_n^g\right) \left(\mathbf{H}_n^g\right)^{\mathrm{H}} (\mathbf{q}$$

where $\operatorname{cov}(\bar{\mathbf{x}}^g_n) \in \mathbb{R}^{T\times T}$ is defined in (24). Once the new statistics of $\hat{x}^g_t(n)$ are obtained, the same procedures explained in Subsection IV-B are followed to determine the active indices and M-ary constellation symbols where the corresponding LLR values are calculated for this case

as

ISSN: 2057-5688

$$\lambda_t^g(n) = \ln\left(\sum_{m=1}^{M} \exp\left(-\frac{\left|\hat{x}_t^g(n\right.}{}\right.\right.$$

According to the MMSE-LLR-OSIC detection, once the estimate $(x^g{}_t)_{\text{MMSE}}$ is obtained, the received signal vectors are updated for $n = 1,2,...,N$ as $\bar{\mathbf{y}}_n^g = \bar{\mathbf{y}}_n^g - \mathbf{H}^g{}_n(\bar{\mathbf{x}}_n^g)_{\text{MMSE}}$ where $(\bar{\mathbf{x}}^g{}_n)_{\text{MMSE}}$ is an all-zero vector except its tth element being $(x^g{}_t(n))_{\text{MMSE}}$ and $(\mathbf{H}^g{}_n)_{*t}$,$n = 1,2,...,N$ are filled with zeros according to SIC principle. The above procedures are repeated until all OFDM-

IM subblocks are demodulated.

TABLE II

DECODING COMPLEXITY COMPARISONS IN TERMS OF TOTAL NUMBER OF COMPLEX MULTIPLICATIONS (CMS)

PERFORMED PER SUBCARRIER

Detector	*MIMO-OFDM*	*MIMO-OFDM-IM*
Brute-Force ML	$R(T+1)M^T \sim O(M^T)$	$R(T+1)(CM^K)^T \sim O(M^{KT})$
Near-ML	n/a	$R(T+1)(M+1)^T \sim O(M^T)$
MMSE (Simple)	$T^3 + 2T^2R + T(R+M) \sim O(M)$	$2T^3 + 5T^2R + TR + CM^K \sim O(M^K)$
MMSE-LLR	n/a	$2T^3 + 5T^2R + T(R+M+1) \sim O(M)$
MMSE(-LLR)-OSIC	$<T^3+T^3(2R+3)+2T^2(R+1)+T(2R+M) \sim O(M)$	$<T^4+T^3(2R+3)+T^2(4R+3)+T(3R+M+1) \sim O(M)$
Spectral Efficiency	$(TN_F \log_2 M)/(N_F + C_p)$	$(NT(\lfloor\log_2(C(N,K))\rfloor + K\log_2 M))/(K(N_F+C_p))$

ISSN: 2057-5688

V. SIMULATION RESULTS AND COMPARISONS

In this section, we present our theoretical as well as Monte Carlo simulation results for the MIMO-OFDM-IM scheme and make comparisons with the classical V-BLAST type MIMOOFDM scheme for different type of detectors and system configurations. The considered OFDM system parameters are given as follows: N_F = 512, subcarrier spacing Δ_f= 15 kHz, sampling frequency f_s = 7.68 MHz, C_p = 36 and L = 10.

In Table II, the decoding complexities of MIMO-OFDM and MIMO-OFDM-IM schemes are given in terms of total number of CMs performed per subcarrier for different type of detectors. As seen from Table II, near-ML, MMSE-LLR and MMSE-LLR-OSIC detectors of MIMO-OFDM-IM have the same order decoding complexity compared to brute-force ML, MMSE and MMSE-OSIC detectors of classical MIMO-OFDM, respectively[4].

In Fig. 3, we compare the BER performance of the MIMO-OFDM-IM scheme for N = 4,K = 2 (Table I) with classical V-BLAST-OFDM using ML detectors and BPSK modulation. Two MIMO configurations are considered: 2×2 and 4×4, where both schemes achieve the same spectral efficiency values of 1.87 and 3.74 bits/s/Hz for these configurations, respectively. As seen from Fig. 3, using ML detection, a diversity order of R is obtained for both schemes, and MIMO-OFDM-IM scheme provides considerable improvements in BER performance compared to classical V-BLAST-OFDM. It should be noted that the proposed near-ML detector outperformed by the brute-force ML detector by a small margin; however, it still exhibits considerably better BER performance than the classical V-BLAST-OFDM. We also observe that the derived theoretical upper in (16) becomes very tight with the computer simulation curves as the SNR increases.

In Fig. 4, we present the BER performance of the MIMO-OFDM-IM scheme for N = 4,K = 3 and classical V-BLAST-OFDM using MMSE type detectors and QPSK modulation. 2×2 and 4×4 MIMO configurations are considered, where both schemes achieve the same spectral efficiency values of 3.74 and 7.48 bits/s/Hz for these configurations, respectively. As seen from Fig. 4, the simple MMSE and MMSE-LLR detectors provides almost the same BER performance for the MIMO-

OFDM-IM scheme while they outperform classical V-BLAST-OFDM using MMSE detection. As expected, the theoretical ABEP curve which is based on the UPEP formula of (29) (exponentially distributed Z_n's) provides a BER performance benchmark, while a much accurate ABEP curve can be obtained by using the semi-analytical UPEP calculation approach of (31). For comparison, the performance of OSIC based MMSE detectors are also shown in Fig. 4. As seen from Fig. 4, for the 2×2 MIMO case, OSIC provides an SNR gain for both schemes; while for the 4 × 4 MIMO case, the interference nulling becomes more dominant and a considerable improvement is observed in BER performance while MIMO-OFDM-IM still outperforms the reference V-BLAST-OFDM scheme with increasing SNR.

Fig. 5 presents the interesting trade-off provided by the MIMO-OFDM-IM scheme between BER performance and spectral efficiency for a 4×4 MIMO system with MMSE-LLR detection. For the selection of active indices, we use the combinatorial number theory method [10], where different N and K values are considered. As seen from Fig. 5, for the same spectral efficiency, the MIMO-OFDM-IM scheme with $M = 8, N = 16, K = 13$ provides approximately 3 dB better BER performance than the reference V-BLAST-OFDM scheme for a BER value of 10^{-5}. On the other hand, as seen from Fig. 5, MIMO-OFDM-IM has the flexibility of adjusting the spectral efficiency by changing the number of active subcarriers K in a subblock, and can achieve better or worse BER performance than the reference MIMO-OFDM-IM scheme with 11.2 bits/s/Hz spectral efficiency. It should be noted that the BER performance of MIMO-OFDM-IM degrades when 64-QAM is employed; however, a better BER performance than classical V-BLAST-OFDM is obtained for all other cases even with a higher spectral efficiency. The price paid for this improvement is the slightly increased signal processing at the receiver for the detection of data

ISSN: 2057-5688

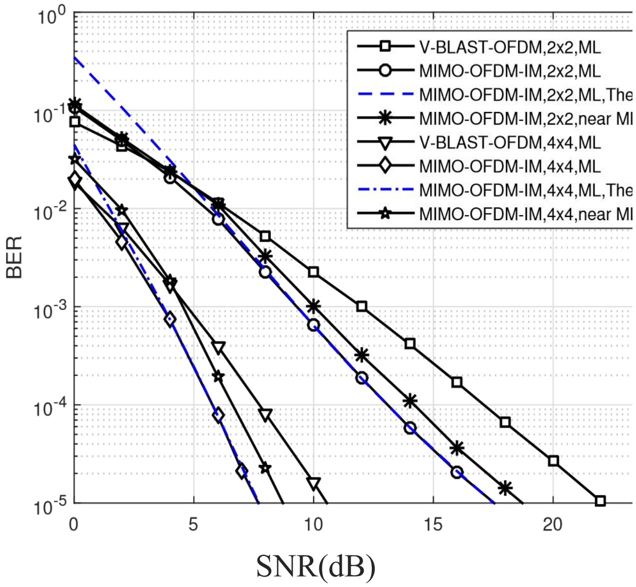

Fig. 3. Performance comparison of V-BLAST-OFDM and MIMO-OFDM-IM (N = 4,K = 2) for BPSK modulation (M = 2), ML/near-ML detection

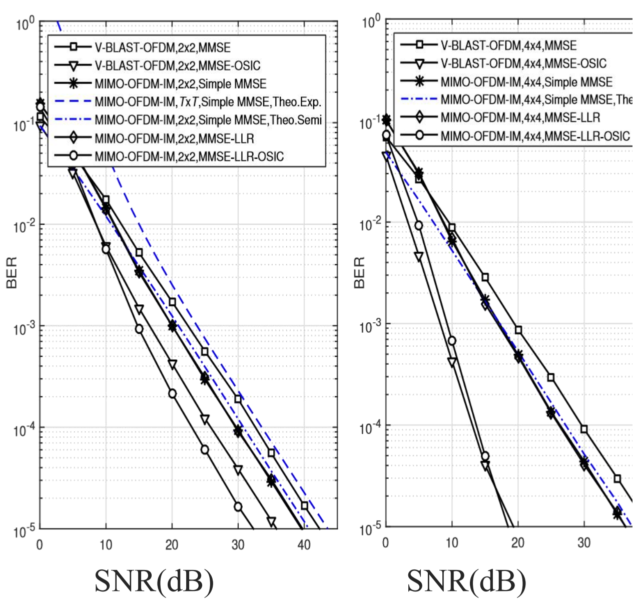

Fig. 4. Performance comparison of V-BLAST-OFDM and MIMO-OFDM-IM (N = 4,K = 3 with reference look-up table) for QPSK modulation (M = 4), simple MMSE, MMSE-LLR, MMSE-LLR-OSIC detection

symbols and active indices.

Finally, we investigate the effects of a realistic channel model and imperfect channel estimation on the performance of the MIMO-OFDM-IM and make comparisons with classical V-BLASTOFDM and Alamouti-OFDM in Fig. 6. Three MIMO configurations are considered: 2 × 4 and

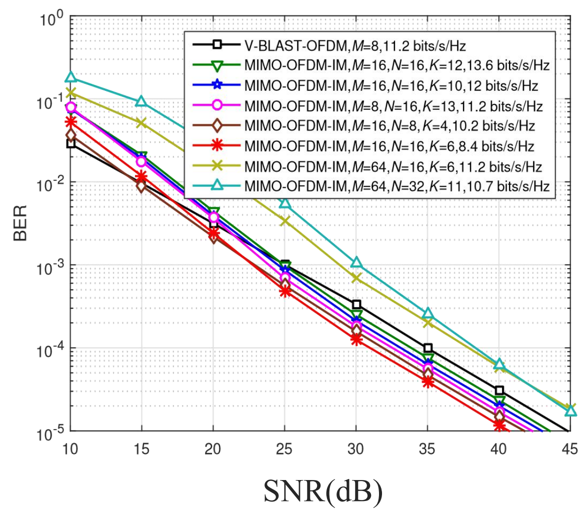

Fig. 5. Performance comparison of V-BLAST-OFDM and MIMO-OFDM-IM for different N, K and M values and for a 4×4 MIMO system with MMSE-LLR detection

INTERNATIONAL JOURNAL OF TECHNO-ENGINEERING
IJTE
ISSN: 2057-5688

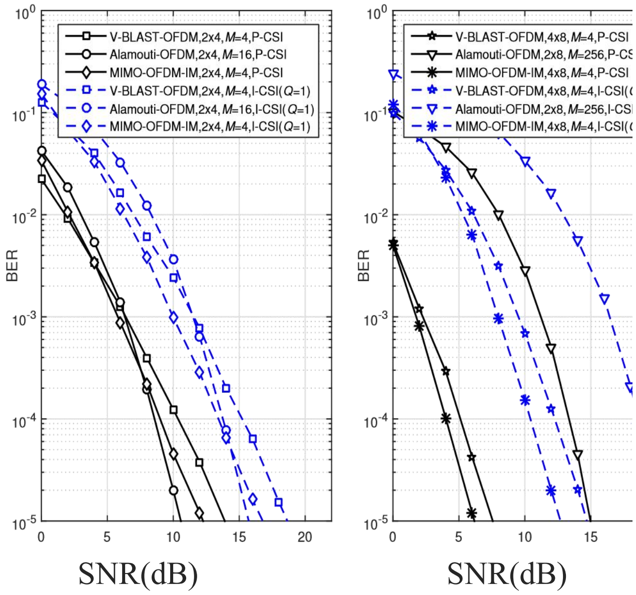

Fig. 6. Performance comparison of V-BLAST-OFDM, Alamouti-OFDM and MIMO-OFDM-IM ($N = 4, K = 3$) at 3.74 and 7.48 bits/sec/Hz for P-CSI and I-CSI ($Q = 1$) cases with MMSE-LLR detection

2/4×8, where all schemes achieve the same spectral efficiency values of 3.74 and 7.48 bits/s/Hz for these configurations, respectively. The considered CIR with $L = 4$ taps is based on Extended Pedestrian A (EPA) model [30] where the corresponding power delay profile is undersampled as in [31] according with the sampling rate of the considered LTE-like system with f_s = 7.68 MHz

TABLE III

CHANNEL IMPULSE RESPONSE BASED ON LTE-EPA MODEL

Linear Tap Gain	0.7594	0.6486	0	0.0517
Tap Delay (*ns*)	0	130	260	390

[30]. In Table III, the normalized CIR values (with total power of unity) used in the simulations are given. In our computer simulations, each tap of the CIR is multiplied by an independent complex Gaussian r.v. with variance 0.5 per dimension. We consider that the channel estimator at the receiver provides an estimate of the channel coefficients as [32] $\hat{\mathbf{H}}^{g}_{n} = \mathbf{H}^{g}_{n} + \mathbf{E}^{g}_{n}$ where the elements of $\mathbf{E}^{g}_{n}$ follow CN $(0,\sigma_e^2)$ distribution. In this study, we assume that the power of

channel estimation errors σ_e^2 decreases with the increasing SNR, i.e., $N_{0,F}$ and σ_e^2 are related via

$Q = N_{0,F}/\sigma_e^2$. For the detection, the receiver considers the mismatched decision metrics where

$\hat{\mathbf{H}}^{g}_{n}$ is used instead of $\mathbf{H}^{g}_{n}$ for all schemes.

As seen from Fig. 6, the BER performance of all systems considerably suffer from imperfect channel estimation (Q = 1) and similar levels of degradation are observed for all schemes. It is interesting to note that Alamouti-OFDM scheme achieves the best BER performance with increasing SNR values for the first configuration. On the other hand, its BER performance degrades considerably with increasing spectral efficiency due to the employment of a higher order constellation, and MIMO-OFDM-IM achieves the best BER performance for the second configuration.

VI. CONCLUSIONS

In this study, the recently proposed MIMO-OFDM-IM scheme has been investigated for next generation 5G wireless networks. For the MIMO-OFDM-IM scheme, new detector types such as ML, near-ML, simple MMSE, MMSE-LLR-OSIC detectors have been proposed and their ABEP have been theoretically examined. It has been shown via extensive computer simulations that MIMO-OFDM-IM scheme provides an interesting trade-off between complexity, spectral efficiency and error performance compared to classical MIMO-OFDM scheme and it can be considered as a possible candidate for 5G wireless networks. The main features of MIMOOFDM-IM can be summarized as follows: i) better BER performance, ii) flexible system design with variable number of active OFDM subcarriers and iii) better compatibility to higher MIMO setups. However, interesting topics such as diversity methods, generalized OFDM-IM cases, high mobility implementation and transmit antenna indices selection still remain to be investigated
for the MIMO-OFDM-IM scheme.

REFERENCES

[1] [1]. G. Jagga Rao, Y. Chalapathi Rao " Robust Bit Error Rate Optimization for MASSIVE MIMOCEM System using Channel Coding Method "in Volume 8-Issue 4S2, pp. 180-184, March 2019.

[2] [2]. M Sumalatha,Dr. P V Naganjaneyulu, and K Satya Prasad ―Low-Power and Area-Efficient FIR Filter Implementation Using CSLA with BEC‖ Journal of Microelectronics, Electromagnetics and Telecommunications,https://doi.org/10. 1007/978-981-10-7329-8_14 Jan-2018,Volume -8 , Issue -3 ,ISSN: 0976-4860,pages:137-142, Springer.

[3] [3]. A. Ravi,Dr. P. V. Naganjaneyulu ,Dr.M.N. Giriprasad ―SAR images denoising using a novel stochastic diffusion wavelet scheme‖,Springer, Cluster Computing Journal ,USA,July-2017,DOI 10.1007/s10586-017-1001-6,ISSN:1573-7543,Pages:01-09,Springer.

[4] [4]. P SekharBabu,Dr. P V Naganjaneyulu, and K Satya Prasad ―Adaptive Beam Forming of MIMO System using Low Complex Selection of Steering Vector‖ International Journal of Advancements in Technology,Jan-

2017,Volume -8 , Issue -3 ,ISSN: 0976-4860,pages:01-06, Elsevier.

[5] [5]. D. Rajendra Prasad, Dr. P. V. Naganjaneyulu ,Dr. K. Satya Prasad ―A Hybrid Swarm Optimization for Energy Efficient Clustering in Multi-hop Wireless Sensor Network‖ Wireless PersCommun DOI 10.1007/s11277-016-3562-8 Springer Science+Business Media New York 2016, Pages:2459-2471.

[6] [6]. P. Ravikumar, P.V. Naganjaneyulu, K. Satya Prasad ―Peak to Average Power Ratio reduction method for Orthogonal Frequency Division Multiplexing in 4G Communication‖, I J C T A, 8(5), 2015, pp. 1703-1708m.

[7] [7]. M Sumalatha, Dr.P .V .NaganjaneyuluandDr.K .Satya Prasad ―ADVANCED FAST FOURIER TRANSFORM USING RADIX-8 BOOTH MULTIPLIER‖ ISSN 2319 - 2518 Int. J. Elec&Electr.Eng& Telecoms. 2015, Special Issue, Vol. 1, No. 3,pp (27-32) November 2015.(Impact factor – 0.454).

[8] [8]. U.Sreenivasulu, Dr. P.V.Naganjaneyulu, ―Performance of bit-interleaved coded multiantenna OFDMA systems over space-frequency‖ National Conference on Advanced Communication Systems &Applications,held at Madanapalli 0n June 2013 , INDIA proceedings pp.161-168.

[9] [9]. T.Srinivas,Dr.P.V.Naganjaneyulu,P.SandeepMohan,R.Shiva Shankar ,Ch.Surender Reddy ―Face Recognition Using PCA and Bit-Plane Slicing‖ PEIE 2012, LNEE, Springer-Verlag Berlin Heidelberg 2012 , pages: 401-407, 2012.

[10] [10]. G. Jagga Rao, Y. Chalapathi Rao, Dr. Anupama Desh Pande "Detection For 6G-NOMA Based Machine Learning Optimization for Successive Adaptive Matching Pursuit Analysis", Q3, pp. 1803-1812, Jan 2020.

[11] [11]. P.V. Naganjaneyulu, Dr.K.Satya Prasad, An adaptive blind channel estimation for OFDM system multimedia by improved H∞ approach (for high data rate)‖, International conference on computer intelligence and multimedia applications held at Siva Kasi on Dec. 2008, vol.4, pages:252-256, Dec. 2008, Published also in IEEE computer society in the portal.acm.in.

[12] [12]. P.V. Naganjaneyulu, Dr.K.Satya Prasad, ―An adaptive blind channel estimation for OFDM system by improved H∞ approach‖, International Conferences on advanced communication systems held at CIT Coimbatore on Oct. 2007, preceding pages:33-36.

[13] [13]. Dr. k. Raju, A. Sampath Dakshina Murthy, Dr. B. Chinna Rao,G. Jagga Rao "A Robust and Accurate Video Watermarking System Based On SVD Hybridation For Performance Assessment" International Journal of Engineering Trends and Technology

ISSN: 2057-5688

(IJETT) – Volume 68 Issue 7 - July 2020.

[14] [14]. P.V. Naganjaneyulu, Dr.K.Satya Prasad, ―A Study of blind channel estimation in OFDM system by H∞ approach‖, National conference on Communication and signal processing held at IEEE, Mumbai on Feb 2007, NCCSP-07, pages:20-24, Feb. 2007.

[15]

[16]

[17] M. Wen, X. Cheng, and L. Yang, "Optimizing the energy efficiency of OFDM with index modulation," in *IEEE Int. Conf. Commun. Systems*, Nov. 2014, pp. 31–35.

[18] W. Li, H. Zhao, C. Zhang, L. Zhao, and R. Wang, "Generalized selecting sub-carrier modulation scheme in OFDM system," in *IEEE Int. Conf. Commun. Workshops*, Jun. 2014, pp. 907–911.

[19] Y. Xiao, S. Wang, L. Dan, X. Lei, P. Yang, and W. Xiang, "OFDM with interleaved subcarrier-index modulation," *IEEE Commun. Lett.*, vol. 18, no. 8, pp. 1447–1450, Aug. 2014.

[20] X. Cheng, M. Wen, L. Yang, and Y. Li, "Index modulated OFDM with interleaved grouping for V2X communications," in *IEEE Int. Conf. Intelligent Transportation Systems*, Oct. 2014, pp. 1097–1104.

[21] E. Basar, "OFDM with index modulation using coordinate interleaving," *IEEE Wireless Commun. Lett.*, vol. 4, no. 4, pp. 381–384, Aug. 2015.

[22] M. Wen, X. Cheng, M. Ma, B. Jiao, and H. V. Poor, "On the achievable rate of OFDM with index modulation," *IEEE Trans. Signal Process.*, vol. 64, no. 8, pp. 1919–1932, Apr. 2016.

[23] B. Zheng, F. Chen, M. Wen, F. Ji, H. Yu, and Y. Liu, "Low-complexity ML detector and performance analysis for OFDM with in-phase/quadrature index modulation," *IEEE Commun. Lett.*, vol. 19, no. 11, pp. 1893–1896, Nov. 2015.

[24] E. Basar, "Multiple-input multiple-output OFDM with index modulation," *IEEE Signal Process. Lett.*, vol. 22, no. 12, pp. 2259–2263, Dec. 2015.

[25] J. Andrews, S. Buzzi, W. Choi, S. Hanly, A. Lozano, A. Soong, and J. Zhang, "What will 5G be?" *IEEE J. Sel. Areas Commun.*, vol. 32, no. 6, pp. 1065–1082, Jun. 2014.

[26] M. Simon and M. S. Alaouni, *Digital Communications over Fading Channels*. New York: John Wiley & Sons, 2005.

[27] G. L. Turin, "The characteristic function of Hermitian quadratic forms in complex normal variables," *Biometrika*, vol. 47,

ISSN: 2057-5688

no. 1/2, pp. 199–201, Jun. 1960.

[28] H. Jafarkhani, *Space-Time Coding*. Cambridge, UK: Cambridge University Press, 2005.

[29] Y. Jiang, M. Varanasi, and J. Li, "Performance analysis of ZF and MMSE equalizers for MIMO systems: An in-depth study of the high SNR regime," *IEEE Trans. Inf. Theory*, vol. 57, no. 4, pp. 2008–2026, Apr. 2011.

[30] H. Andersen, M. Hojbjerre, D. Sorensen, and P. Eriksen, *Linear and Graphical Models for the Multivariate Complex Normal Distribution*. Springer-Verlag New York, Inc., 1995.

[31] R. Bohnke, D. Wubben, V. Kuhn, and K.-D. Kammeyer, "Reduced complexity MMSE detection for BLAST architectures," in *IEEE Global Commun. Conf.*, vol. 4, Dec. 2003, pp. 2258–2262.

[32] M. B. Stefania Sesia, Issam Toufik, *LTE The UMTS Long Term Evolution, From Theory to Practice*.John Wiley & Sons, 2014.

[33] *Universal Mobile Telecommunications System (UMTS); Deployment aspects (3GPP TR 25.943 version 12.0.0 Release 12)*, 2014.

[34] V. Tarokh, A. Naguib, N. Seshadri, and A. R. Calderbank, "Space-time codes for high data rate wireless communication: Performance criteria in the presence of channel estimation errors, mobility, and multiple paths," *IEEE Trans. Commun.*, vol. 47, no. 2, pp. 199–207, Feb. 1999.